Magnesium Technology 2013
Edited by: Norbert Hort, Suveen N. Mathaudhu, Neale R. Neelameggham, and Martyn Alderman
TMS (The Minerals, Metals & Materials Society), 2013

Thermodynamics of phase formation in Mg-La-Ce-Nd alloys

Rainer Schmid-Fetzer[1], Joachim Gröbner[1], Artem Kozlov[1], Milan Hampl[1],
Mark A. Easton[2], Suming Zhu[2], Mark A. Gibson[3] and Jian-Feng Nie[2]

[1]Institute of Metallurgy, Clausthal University of Technology, Robert-Koch-Str. 42, D-38678 Clausthal-Zellerfeld, Germany
[2]CAST CRC, Department of Materials Engineering, Monash University, Victoria 3800, Australia
[3]CAST CRC, CSIRO Process Science & Engineering, Clayton, Victoria 3169, Australia

Keywords: Simulation, Rare earth, Phase Diagrams, Thermodynamics, Solidification paths

Abstract

Experimentally validated thermodynamic descriptions have been developed for the ternary Mg-La-Ce, Mg-La-Nd, and Mg-Ce-Nd systems by selecting key alloys in both systems and analyzing the phase formation in both the as-cast and heat treated state by SEM/EDS and DSC. These results were combined to form the validated thermodynamic Calphad-type description for quaternary Mg-La-Ce-Nd alloys. It is shown that for these light rare earth elements (La, Ce, Nd) the intermetallic phases with Mg exhibit significant mutual solid solubility in the ternary systems, extending into the quaternary alloy system. This is reflected by considering the shared crystal structures in the thermodynamic modeling. Simulated solidification paths of three Mg-La-Ce-Nd alloys with different La:Ce:Nd ratios and a common total content of 5 wt.% rare earth (RE) metals are evaluated using computational thermodynamics. Unexpected and distinctly different solidification behavior of these three alloys is revealed. The sequence La→Ce→Nd in the periodic table is not at all reflected in a monotonous solidification behavior. The demonstrated individual impact of each of these elements forbids treating the RE additions as a mere wt.% sum of RE elements.

Introduction

In recent years there has been considerable interest in the addition of RE metals to magnesium and its alloys to improve the mechanical properties, high temperature creep resistance in particular. The RE elements are generally added to Mg alloys in the form of mischmetal, a mixture of various RE metals. Commonly used mischmetal consists mainly of the light RE metals, i.e. La (25-34%), Ce (48-55%), Nd (11-17%) and small amounts of Pr and Sm. It has been realized that the individual RE elements may exert distinctly different effects on the mechanical properties of Mg alloys [1-3].

The purpose of this work is to present a concise comparison of the key features of the three ternary subsystems at the Mg-corner of the Mg-La-Ce-Nd quaternary phase diagram and to apply our validated knowledge of this system in solidification and heat treatment simulations of quaternary Mg-La-Ce-Nd alloys with different ratios of RE additions.

Phase diagrams of ternary Mg-RE-RE systems

The first ternary system of Mg with two light rare earths elements investigated by the present authors was the Mg-Ce-Nd system [1]. Easton et al. [2] have elaborated the crystallographic and thermodynamic effects on phase selection in binary magnesium-rare earth (Ce or Nd) alloys. Subsequently the addition of La was investigated in the two ternary Mg-Ce-La and Mg-La-Nd systems by Gröbner et al. [3].

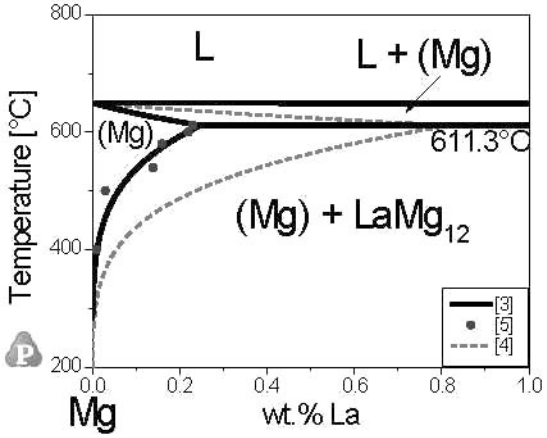

Figure 1: The Mg-rich part of the Mg-La binary phase diagram based on our recent assessment [3] compares well with the experimental data for the solvus of (Mg) by Rokhlin [4] and significantly differs from the calculation by Guo and Du [5].

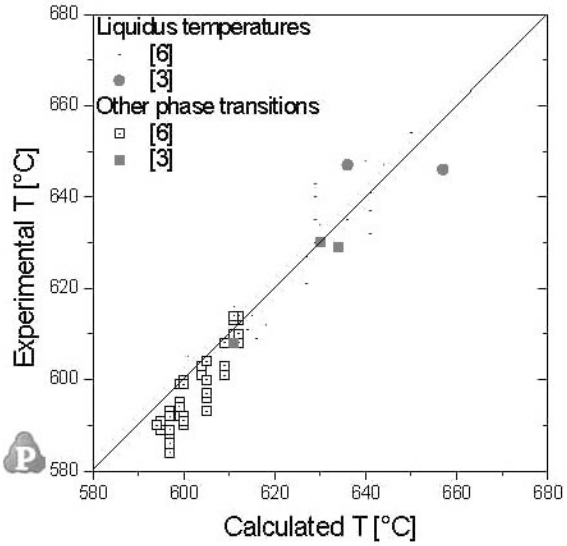

Figure 2: Comparison of all experimentally observed thermal signals in the Mg-La-Ce system [6, 3] with temperatures from the thermodynamic calculation of [3].

The binary phase diagram Mg-La was also re-assessed in that work [3] and its Mg-rich part is shown in Fig. 1. The focus is on

the solid solubility of La in (Mg). Our calculated solvus data agree with the experimental data Rokhlin [4] whereas the calculated data by Guo and Du [5] are about four times larger at the eutectic temperature of 611.3°C.

For ternary Mg-La-Ce alloys the experimental thermal signals for samples on six vertical sections at constant 95, 90, 85, 80, 75 and 70 wt.% Mg were reported by Rokhlin and Bochvar [6] and additional DSC experiments were performed for selected key alloys in our previous work [3]. Figure 2 shows the comparison between the experimental thermal signal temperatures and those calculated for all these alloys from the thermodynamic description by Gröbner et al. [3]. Essentially, the agreement is better than ±10 K which may be considered satisfactory in view of the experimental challenges for the Mg-RE systems.

The calculated Mg-rich parts of the liquidus projections of the three ternary subsystems at the Mg-corner of the Mg-La-Ce-Nd quaternary are shown in Figs. 3(a–c), based on our recently obtained data [1, 3]. A large extension of the primary crystallization field of (Mg) up to 15 wt.% RE or more is noted, way beyond the typical alloying additions of RE in applied magnesium alloys. The Mg-richest intermetallic phase in all those ternary systems is $REMg_{12}$, denoting the solid solution phase $(La,Ce,Nd)Mg_{12}$. Its liquidus surface intersects that of (Mg) in the monovariant equilibrium Liquid + (Mg) + $REMg_{12}$, except for alloys very close to the Mg-Nd binary edge where the RE_5Mg_{41} phase appears, forming the monovariant equilibrium Liquid + (Mg) + RE_5Mg_{41}. In most of the Mg-rich ternary alloys depicted in Figs. 3(a–c) $REMg_{12}$ is expected to solidify as a stable second phase after primary solidification of (Mg). The exception being alloys with a high Nd/(La+Ce) ratio where RE_5Mg_{41} is expected to solidify as a stable second phase. The problem of retarded nucleation of the stable Nd_5Mg_{41} phase in binary hypoeutectic Mg-Nd cast alloys, which tend to contain $NdMg_{12}$ at quite slow cooling rates or $NdMg_3$ if the cooling rate is particularly rapid, has been solved recently [2]. It will be addressed for a quaternary Nd-rich alloy later in this study.

In Figs. 4(a-c) the calculated Mg-rich parts of the isothermal phase diagram sections at 500°C of the three ternary systems are compared. The phases REMg (structure type cP2-CsCl) and $REMg_3$ (cF16-BiF_3) exhibit complete solid solution ranges in all three ternaries. Moving closer to the Mg-corner the intermetallics RE_5Mg_{41} (tI92-Ce_5Mg_{41}), RE_2Mg_{17} (hP38-$Ni_{17}Th_2$), and $REMg_{12}$ (tI26-$ThMn_{12}$) may exhibit limited or complete solid solution ranges as clearly indicated in Figs. 4(a-c). The intricacies of modeling such intermetallic solution phase in a wider perspective of the extensive thermodynamic Mg alloy database are recently detailed elsewhere [7].

The single-phase region of (Mg) is highlighted by the red colored regions in the ternary phase diagrams at 500°C, but just visible as a dot in Fig. 4(a) and as a narrow line in Figs. 4(b) and (c). That is due to the small solid solubilities in the binary systems at 500°C: 0.06 wt.% La, 0.2 wt.% Ce, and 2.2 wt.% Nd in the binary (Mg) phases, respectively.

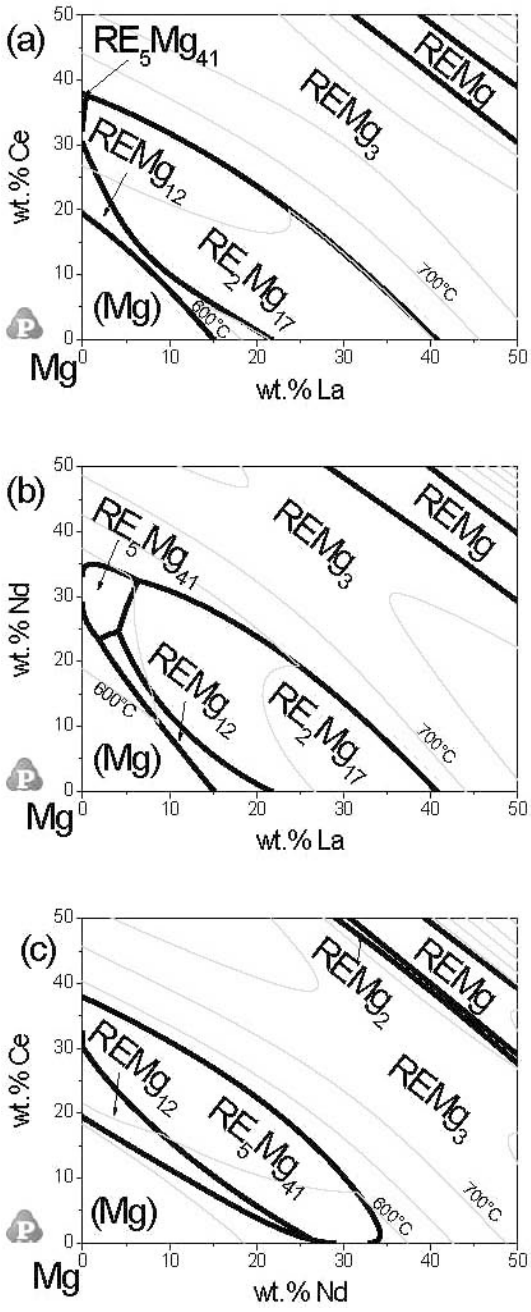

Figure 3. Calculated Mg-rich part of the liquidus projections of three ternary Mg-RE-RE systems: (a) Mg-La-Ce, (b) Mg-La-Nd, (c) Mg-Ce-Nd.

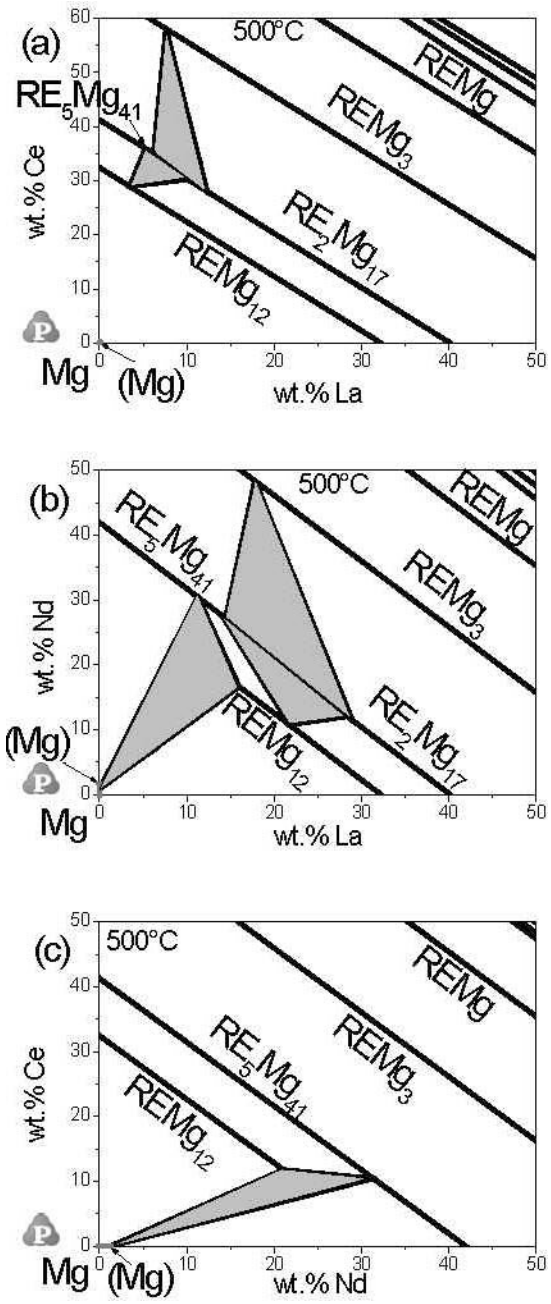

Figure 4. Calculated Mg-rich part of the isothermal sections at 500°C of three ternary Mg-RE-RE systems: (a) Mg-La-Ce, (b) Mg-La-Nd, (c) Mg-Ce-Nd. Triangular three-phase regions are gray-shaded and the single-phase (Mg) solid solution range is highlighted by red color.

Solidification and heat treatment simulation of quaternary Mg-La-Ce-Nd alloys with different ratios of RE additions

Based on our validated assessments of the ternary subsystems and the consistent description of the multicomponent intermetallic solution phases the phase formation in quaternary Mg-La-Ce-Nd alloys can be reliably predicted by thermodynamic calculations. This is exemplified on three alloys with a total addition of 5 wt.% RE but different ratios of La:Ce:Nd. The three alloys investigated are denoted as "3-1-1", "1-3-1", and "1-1-3" with the compositions 3La-1Ce-1Nd (wt.%), 1La-3Ce-1Nd (wt.%), and 1La-1Ce-3Nd (wt.%), respectively. Their location in the quaternary system is sketched in Fig. 5. The intention is to study the impact of variations in the RE composition of alloying additions such as mischmetal.

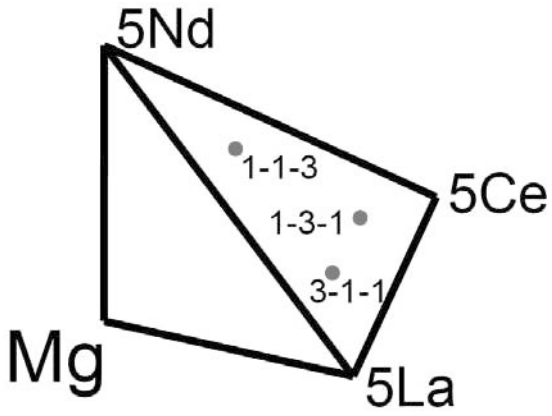

Figure 5: Perspective sketch of the Mg-rich corner of the Mg-Ce-La-Nd quaternary system sectioned at the 95 wt.% Mg plane, showing the locations of the three investigated alloys: Alloy 3-1-1 with 3La-1Ce-1Nd (wt.%), alloy 1-3-1 with 1La-3Ce-1Nd (wt.%), and alloy 1-1-3 with 1La-1Ce-3Nd (wt.%).

All thermodynamic calculations are performed using the Pandat software [8] and the new and significantly upgraded PanMg2012 database [7, 9] (www.computherm.com).

The constitution of the as-cast alloys is approximately simulated using Scheil solidification conditions and the developing phase amounts are given in Figs. 6(a-c). The final amount of intermetallic phases at the Scheil solidus, considered to constitute the frozen-in microstructure, is denoted in the diagrams, e.g. 9.2% of $REMg_{12}$ phase and 1.5% of RE_5Mg_{41} phase in alloy 3-1-1. The at.% scale based on moles of atoms of all phases is used (and not the phase weight fraction) since it is often a better approximation to the volume fraction of the phases in the microstructure.

The complex compositions of these $(La,Ce,Nd)Mg_{12}$ and $(La,Ce,Nd)_5Mg_{41}$ phases, also resulting from the calculations, are not reported here but may be envisaged from the extended solubility ranges in the ternary subsystems shown for 500°C in Figs. 4(a-c). The total amount of intermetallic phases reported in Figs. 6(a-c) decreases from 10.7%→9.5%→7. 8% if the majority RE component changes from La→Ce→Nd. In the same sequence the dominating $REMg_{12}$ phase is replaced by the RE_5Mg_{41} phase. That interdependence could only be revealed by the quantitative thermodynamic simulation considering all the quaternary solubilities in the intermetallics and in the (Mg) phase as well as the quaternary liquidus properly.

The sequence La→Ce→Nd reflects the increasing order of these elements in the periodic table. One might, thus, be tempted to assume a monotonous change in the solidification behavior, as already suggested by the monotonously decreasing

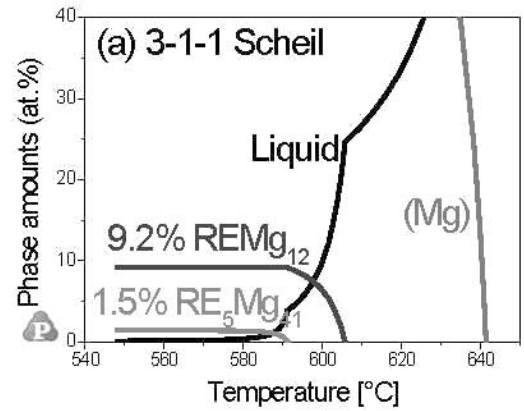

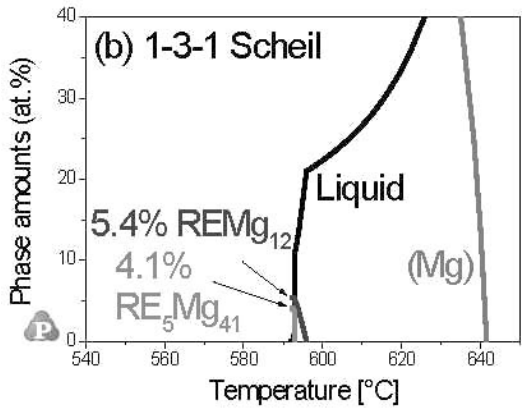

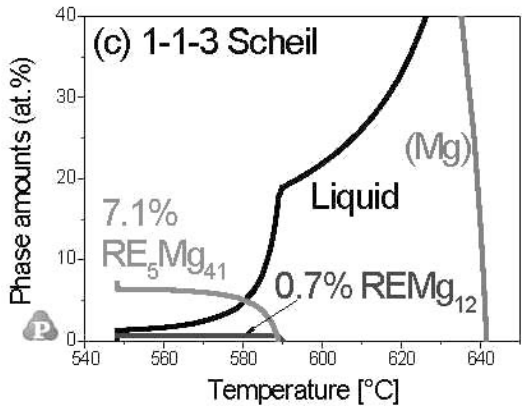

Figure 6. Calculated phase amounts during Scheil solidification simulation of the three Mg-La-Ce-Nd alloys detailed in Figure 5: (a) Alloy 3-1-1, (b) Alloy 1-3-1, (c) Alloy 1-1-3.

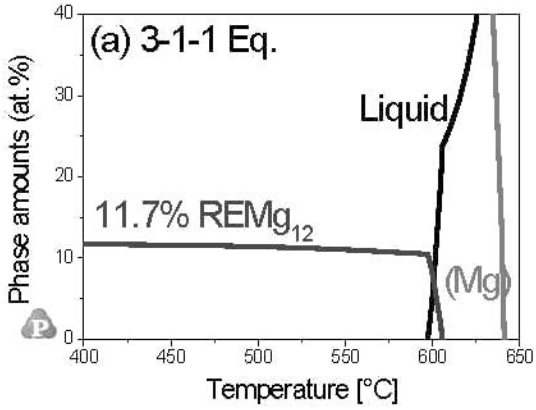

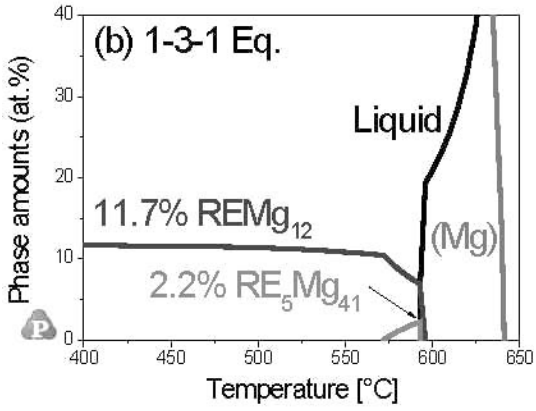

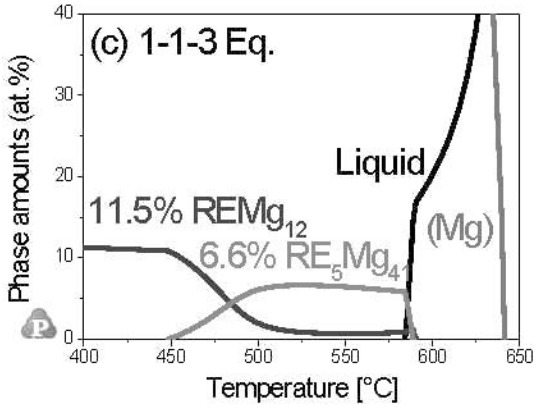

Figure 7. Calculated phase amounts at equilibrium for the three Mg-La-Ce-Nd alloys detailed in Figure 5: (a) Alloy 3-1-1, (b) Alloy 1-3-1, (c) Alloy 1-1-3.

total amount of intermetallic phases. That is, however, not the case at all. The Scheil solidus of the "middle" alloy 1-3-1 is much higher, 592°C, compared to the alloys 3-1-1 and 1-1-3, both with 548°C. That gives alloy 1-3-1 a much narrower freezing range since the liquidus temperatures of all three alloys are virtually the same, at 641.5°C. The reason is that alloy 1-3-1 terminates solidification under Scheil conditions with a truly quaternary liquid composition of Mg-0.7La-15.3Ce-4.8Nd (wt.%) and still precipitating according to the monovariant reaction

$$\text{Liquid} \rightarrow (\text{Mg}) + \text{REMg}_{12} + \text{RE}_5\text{Mg}_{41}$$

occurring between 593 and 592°C for this alloy. That is, coincidentally, very close to the equilibrium solidus of this alloy 1-3-1 at 593°C with the same reaction. By stark contrast both alloys 3-1-1 and 1-1-3 terminate Scheil solidification with the binary liquid composition of Mg-28.8Nd (wt.%), which is attained from quaternary liquid compositions while running down the polythermal reaction

$$\text{Liquid} \rightarrow (\text{Mg}) + \text{RE}_5\text{Mg}_{41}$$

from about 578°C down to the binary Mg-Nd eutectic at 548°C. This startling and distinct behavior could not have been envisaged without the tool of computational thermodynamics, even if one had known the graphical presentation of the ternary phase diagrams.

It is noted that in all cases the $REMg_{12}$ phase is the first intermetallic to precipitate in all alloys. The temperature step until the RE_5Mg_{41} phase appears decreases as seen from Figs. 6(a-c).

For comparison the results from equilibrium solidification simulation (Lever rule) for these three alloys are given in Figs. 7(a-c). Again, the $REMg_{12}$ phase is the first intermetallic to precipitate in all alloys. Termination of solidification is somewhat different though, occurring in the following reactions under equilibrium for alloys "3-1-1", "1-3-1", and "1-1-3", respectively:

597°C Liquid → (Mg) + $REMg_{12}$

593°C Liquid → (Mg) + $REMg_{12}$ + RE_5Mg_{41}

584°C Liquid + $REMg_{12}$ → (Mg) + RE_5Mg_{41} .

The subsequent solid state reaction

(Mg) + RE_5Mg_{41} → $REMg_{12}$

occurs in the latter two alloys, and below 450°C $REMg_{12}$ is the only stable intermetallic phase in all three alloys. The maximum intermetallic phase amounts occurring at any temperature is denoted in the diagrams in Figs. 7(a-c). A significant heat treatment response with changing phase amounts is expected. That is seen by comparing the initial phase amounts in the as-cast structures, denoted in Figs. 6(a-c) to the ones expected after long-term heat treatment at selected temperatures in Figs. 7(a-c).

Impact of metastable constrained solidification

It has been shown recently that in Mg-Nd and Mg-Ce-Nd alloys the formation of the stable Nd-rich RE_5Mg_{41} in the as-cast state is easily overrun and that at small supercooling the competing $REMg_{12}$ phase may form instead [1] and that the Nd-rich RE_5Mg_{41} phase develops at high heat treatment temperatures and long enough times. Based on thermodynamic and crystallographic matching calculations, the phase selection is well explained by the competition between the driving force (reduction in bulk Gibbs energy) and the nucleation energy barrier (increment of surface energy) [2].

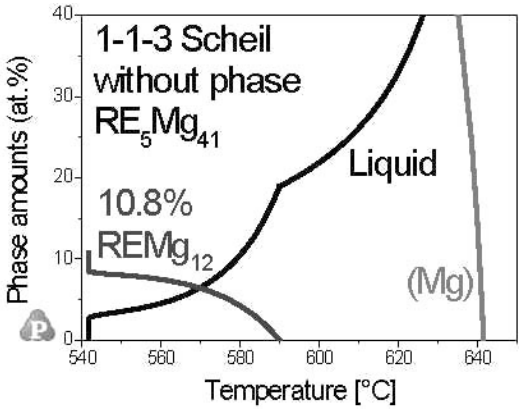

Figure 8. Calculated phase amounts during Scheil solidification simulation of alloy 1-1-3 suppressing the phase RE_5Mg_{41}, compare to Fig. 6(c).

That knowledge is applied to the Nd-richest of the three quaternary alloys, 1-1-3, by simulating such a metastable as-cast state in a Scheil calculation with the RE_5Mg_{41} phase being suspended. The phase selection is constrained by this exclusion; otherwise the Scheil conditions apply which, of course, always generate a metastable constitution in view of the blocked solid state diffusion. The resulting phase amounts are given in Fig. 8. The stable and metastable solidification paths are of course identical until the RE_5Mg_{41} phase precipitates at 589°C, compare with Fig. 6(c). In the stable scenario 1.1% of residual liquid solidify in the stable binary Mg-Nd eutectic:

548°C Liquid → (Mg) + Nd_5Mg_{41} (stable)

In the metastable scenario, Fig. 8, the suppression of the RE_5Mg_{41} phase does not prevent the liquid composition from segregating to the binary Mg-Nd edge, where 2.7% of residual liquid solidify in the metastable binary Mg-Nd eutectic:

541.8°C Liquid → (Mg) + $NdMg_{12}$ (metastable)

Subject to a sufficiently long heat treatment, attaining the equilibrium state, the phases will transform to the constitution shown in Fig. 7(c), irrespective of the conditions assumed for the as-cast state.

Terminal freezing range (TFR)

The key temperatures during the Scheil solidification simulations are listed for the three quaternary Mg-La-Ce-Nd alloys at preset values of fraction solid, f_s, in Table I. In addition to the "Scheil solidus" at f_s = 100% two additional key temperatures are given at the fractions solid of f_s = 88% and f_s = 98%. The temperature difference between these points had been defined as the *terminal freezing range* (TFR) [10]. The idea put forward with this definition is that a small TFR should be beneficial in order to avoid hot tearing. It has been detailed that the value of ΔT-88/98, describing the partial freezing range of the "almost" last 10% of solidifying liquid, is more relevant than ΔT-90/100. That is because the exact termination of solidification, f_s = 100%, cannot generally be expected to be predicted precisely from the limiting Scheil model since the path of the last 2% of liquid may be prone to some artifacts [10]. One might argue about the values of f_s = 88% and f_s = 98% selected here, however, they are located approximately in the region where interdendritic feeding, burst and solid feeding become dominant, triggering casting defects [11]. The concept of TFR [10] has found some interest and was successfully applied to the hot tearing susceptibility of Mg-Zn alloys [12] and the development of high-strength and ductile Mg–Zn–Zr–Ca–Mn(–Yb) alloys [13].

Table I. Temperatures attained during Scheil solidification simulation at preset values of fraction solid, f_s, and the terminal freezing range, **ΔT-88/98,** for the three quaternary Mg-La-Ce-Nd alloys detailed in Figure 5. Their liquidus temperatures vary only between 641.4 and 641.5°C.

Alloy	Temperature at preset f_s [°C]			ΔT-88/98 [K]
	f_s = 88 %	f_s = 98 %	f_s = 100%	
3-1-1	601	589	548	12
1-3-1	593.3	592.8	592.0	0.5
1-1-3	587	564	548	23
1-1-3 *	582	542	542	20

* Constrained phase selection, without RE5Mg41

It is another startling result that these values of ΔT-88/98, given in Table I, are drastically different for the three quaternary alloys

with all the same total RE addition of 5 wt.%. And these values do not even vary monotonously in the sequence La→Ce→Nd of the major RE addition. Again, the "middle" alloy 1-3-1 shows an extremely small value of ΔT-88/98 = 0.5 K. One might thus expect the Ce-rich alloy to perform better during casting compared to the La- and Nd-rich ones.

References

1. J. Gröbner, A. Kozlov, R. Schmid-Fetzer, M. A. Easton, S. Zhu, M. A. Gibson, and J.-F. Nie, "Thermodynamic analysis of as-cast and heat treated microstructures of Mg-Ce-Nd alloys," *Acta Mater.*, 59 (2011) 613-622.
2. M.A. Easton, M.A. Gibson, D. Qiu, S.M. Zhu, J. Gröbner, R. Schmid-Fetzer, and J.F. Nie, M. Zhang, "The role of Crystallography and Thermodynamics on Phase Selection in Binary Magnesium-Rare Earth (Ce or Nd) Alloys," *Acta Mater.*, 60 (2012) 4420-4430.
3. J. Gröbner, M. Hampl, R. Schmid-Fetzer, M.A. Easton, S.M. Zhu, M.A. Gibson, and J.F.Nie, "Phase Analysis of Mg-La-Nd and Mg-La-Ce Alloys," *Intermetallics*, 28 (2012) 92–101.
4. L.L. Rokhlin, "Magnesium Alloys Containing Rare Earth Metals, " Taylor & Francis, London, 2003.
5. C. Guo and Z. Du, "Thermodynamic assessment of the La–Mg system," *J. Alloys Comp.* 385 (2004) 109–113.
6. L.L. Rokhlin, N.R. Bochvar, "Phase Diagrams of the Mg-La-Ce System," *Izv. Akad. Nauk SSSR, Metally*, (2) 193-197 (1977).
7. R. Schmid-Fetzer, J. Gröbner, "Thermodynamic database for Mg alloys — progress in multicomponent modeling," *Metals*, 2 (2012) 377-398. Special Issue "Magnesium Technology", open access.
8. W. Cao, S. Chen, F. Zhang, K. Wu, Y. Yang, Y. Chang, R. Schmid-Fetzer, W. A. Oates, "PANDAT Software with PanEngine, PanOptimizer and PanPrecipitation for Materials Property Simulation of Multi-Component Systems," *Calphad*, 33 (2009) 328-342.
9. J. Gröbner, R. Schmid-Fetzer, "Key issues in a thermodynamic Mg alloy database," *Metall. Mater. Trans. A*, (2012) accepted
10. M.B. Djurdjevic, R. Schmid-Fetzer, "Thermodynamic Calculation as a Tool for Thixoforming Alloy and Process Development," *Mater. Sci. Engin.* A, 417 (2006) 24-33.
11. A.K. Dahle, D.H. StJohn, "Rheological behaviour of the mushy zone and its effect on the formation of casting defects during solidification," Acta Mater., 47 (1998) 31–41.
12. P. Gunde, A. Schiffl, P.J. Uggowitzer, "Influence of yttrium additions on the hot tearing susceptibility of magnesium–zinc alloys," *Mater. Sci. Engin.* A, 527 (2010) 7074–7079.
13. P. Gunde, A.C. Hänzi, A.S. Sologubenko, P.J. Uggowitzer, "High-strength magnesium alloys for degradable implant applications," *Mater. Sci. Engin.* A, 528 (2011) 1047–1054.